IMPACT OF MATERIALS ON CANDU-SCWR LATTICE PHYSICS

J. Pencer, D. Guzonas, G.W.R. Edwards and B. Hyland
Atomic Energy of Canada Limited (AECL) -Chalk River Laboratories
Chalk River, Ontario, Canada

Abstract

One of the key challenges in the development of a CANDU® pressure-tube supercritical water-cooled reactor (SCWR) is the selection of materials appropriate for in-core use. Such materials must be able to withstand the high-temperature, corrosive environment, and effects of irradiation encountered in the core, while at the same time minimizing parasitic neutron absorption. Achieving the appropriate balance between reactor physics and materials requirements necessitates knowledge of both materials properties of candidate alloys and their impact on lattice physics. In this paper, lattice physics calculations have been performed for the CANDU-SCWR for several categories of candidate in-core materials. In addition, a simple relation is derived that can be used to estimate the relative influence of in-core materials on lattice reactivity and fuel discharge burnup, based on material chemical composition and density.

1. Introduction

In 2001, a cooperative international initiative, the Generation IV International Forum (GIF), was formed in order to carry out research and development on potential next generation nuclear energy systems, with specific focus on four generic goals: safety, sustainability (e.g. fuel utilization), economics, and proliferation resistance [1]. Canada's primary contribution to this effort is the development of a CANDU-based pressure-tube (PT) supercritical water-cooled reactor (SCWR). The main advantage of the SCWR over conventional reactor systems is the overall increase of thermal efficiency. The CANDU SCWR is intended to have an operating pressure of 25 MPa; the coolant densities and temperatures range between 615 kg/m^3 and 350 ºC at the inlet and 68 kg/m^3 and 625 ºC, respectively, at the outlet. These parameters lead to an increase in thermal efficiency from about 33% for CANDU reactors to 45%- 50% for a CANDU SCWR using a direct turbine cycle [2]. The use of supercritical water (SCW) as coolant presents major materials challenges [3-15], because of the high temperatures and highly corrosive environment in SCW. The selection of materials appropriate for in-core applications (e.g. fuel cladding) also remains a significant technical issue [9].

Materials currently under consideration for in-core use in the SCWR include austenitic stainless steels, ferritic / martensitic (F-M) steels, oxide dispersion strengthened (ODS) steels, and alloys based on nickel, titanium, or zirconium [3]. Often, materials studies such as those reported in [4-15] do not include the effect of in-core materials on core neutronics as a criteria for materials selection. All potential in-core materials will absorb neutrons to some extent, leading to a decrease in overall fuel efficiency. Zirconium alloys are generally not considered appropriate for use under SCW conditions because it is expected that corrosion rates would be too high and that the material strength would be insufficient. Consequently in-core materials will have to be

® CANDU (CANada Deuterium Uranium) is a registered trademark of Atomic Energy of Canada Limited (AECL)

fabricated from more suitable materials such as stainless steel, which, unfortunately, are also highly neutron absorbing. The resultant increase in parasitic neutron absorption in the core will reduce the exit burnup (in comparison to an equivalent core with zirconium-based in-core materials), or will necessitate higher fuel enrichment to reach a desired target burnup. Both of these consequences lead to potential reductions in effective fuel utilization, one of the GIF's key goals in sustainability [1]. Thus, one of the primary challenges in SCWR development is to find materials durable enough to tolerate SCW conditions, such that gains in thermodynamic efficiency more than offset the losses in fuel efficiency induced by increased neutron absorption in those materials.

The impact of materials on reactivity and fuel exit burnup depends in a complex way on a number of factors such as the spatial distribution of neutrons and their energies, the physical location and distribution of materials, and their neutron-energy-dependent absorption and scattering properties. Consequently, detailed physics calculations (e.g. lattice physics calculations) are required in order to make an assessment of the impact of material selection on fuel exit burnup. Because of the wide variety of potential candidate in-core materials (see, e.g. [3]) and the time and effort required for detailed physics analysis, it is desirable to have an alternative means of estimating material effects on reactivity and fuel exit burnup. In this paper, the possibility of using the thermal neutron absorption cross sections of materials to estimate their impact on reactivity and exit burnup is investigated.

2. Modelling and Analysis Methods

The bundle design used in this paper is shown in Figure 1, and corresponds to the 54-element bundle as described in [10]. This bundle design has three concentric fuel rings, consisting of 12, 18 and 24 identical elements of 4% low enriched uranium (LEU) fuel, a fuel bundle rubber band radius of 6.4 cm, and a large centre pin filled with coolant. The fuel channel is a re-entrant type fuel channel (REC) as described in [11], and consists of a pressure tube and a concentric liner tube (Figure 1). Coolant first flows between the pressure tube and outer liner tube, then, at the end of the channel, is directed through the channel where the fuel resides. As with current CANDU reactors, the pressure tube is separated from the moderator by a gas annulus and calandria tube. For this study, the centre pin was filled with coolant surrounded by a 50% perforated liner tube (the inner liner tube shown in green in Figure 1). The perforations in the liner tube allow exchange between the coolant in the centre pin and the coolant surrounding the bundle. For ease of modeling, the coolant in the centre pin was held at the same density and temperature as the coolant surrounding the bundle. Detailed bundle specifications are given in [10]. Note that the REC design in this work differs somewhat from REC designs presented elsewhere. This difference reflects changes associated with ongoing development of the bundle and channel, and changes in fuel composition.

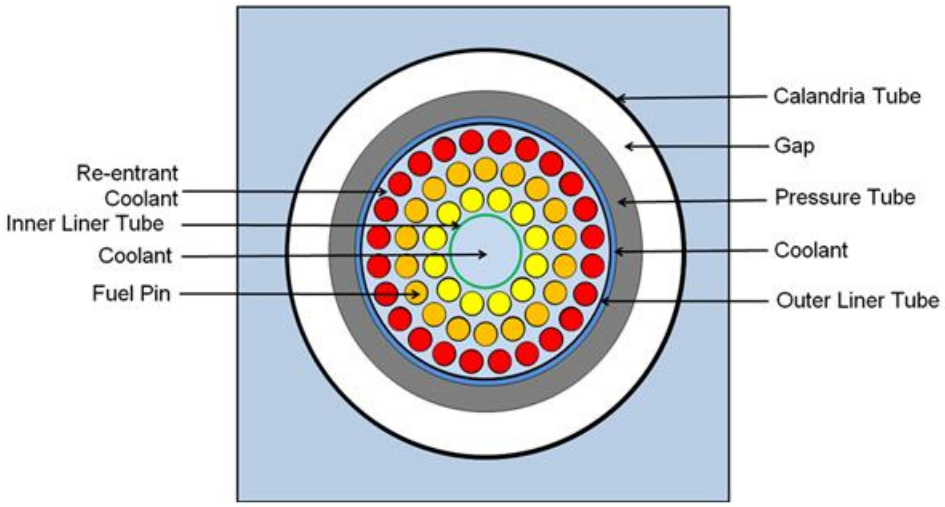

Figure 1 SCWR 54-Element Bundle Design and Re-entrant channel (REC) lattice cell

Lattice physics calculations were performed using WIMS-AECL 3.1, which is a two-dimensional multi-group deterministic lattice physics code that solves the integral neutron transport equation using collision probabilities [12]. For this study, WIMS-AECL was used in conjunction with an 89-group nuclear data library based on ENDF/B-VI [12]. For the results presented here, WIMS-AECL was used to evaluate lattice reactivity as a function of fuel burnup. Fuel channel models in WIMS-AECL consisted of two-dimensional slices through the channels, perpendicular to the channel axis as illustrated in Figure 1. Calculations were performed at the axial position corresponding to the midpoint of the channel, corresponding to a coolant temperature and density of 402 ºC and 0.19 g/cm^3, respectively, based on the coolant temperature and density profile provided in [10]. All other parameters are as specified in [10].

The impact of the choice of in-core materials is assessed in this report using the thermal neutron absorption cross section, the neutron multiplication factor, and the exit burnup. Graves [13] approximates the reactor multiplication factor, $k_{reactor}$, as

$$k_{reactor} = \frac{1}{n}\sum_{i=1}^{n} k_i \,, \qquad (1)$$

where n is the number of fuel batches (each with the same number of fuel bundles), and k_i is the infinite multiplication factor (k-infinity) of batch i. The exit burnup is reached when $k_{reactor}$ reaches 1 plus a constant used to account for the reactivity worth of core leakage and absorption due to in core devices. For continuous refuelling (i.e. the limit as the number of batches, $n \to \infty$), $k_{reactor}$ is determined by integrating k_i over burnup. Here this quantity is referred to as integrated k-infinity. It was assumed that the exit burnup was reached when the integrated k-infinity reached a value of 1.040, where core leakage and absorption were assumed to have a worth of approximately 40 mk (40 mk corresponds to dk/k = 0.040, 4% or 4000 pcm) [10].

The impact on lattice physics of fifteen materials, including austenitic stainless steels (310 SS, 304NG, H2, T3F and T6), F/M steel (P92), ODS steels (16Cr-Al and 14YWT), nickel-based alloy (Inconel 625), titanium based alloy (Ti-15Mo-5Zr-3Al), zirconium-based alloys (Zircaloy-4 and Zr-1.0-Cr-0.2Fe) and superaustenititc stainless steels (Carpenter 20Cb-3,

AL-6XN and Nitronic 50) were investigated. Ten of these materials are candidate SCWR materials, chosen from recent materials studies ([3], [16-21]); the three superaustenitic steels are commonly used in marine, chemical processing and medical industries and show high corrosion resistance; two materials, 310 SS and Zircaloy-4, are currently used as structural material and cladding, respectively [23]. For this study, the materials were used for the fuel cladding, and the inner and outer liner tubes shown in Figure 1. The compositions of the various materials are provided in Table 1.

Table 1
Chemical Compositions (weight %) of Candidate In-Core Materials

	C	Cr	Ni	Zr	Ti	Mo	Other	Balance
310 SS	0.25	25.0	20.5	-	-	-	P:0.045, S:0.030, Si:1.5; Mn:2.0	Fe
304NG [3]	0.018	19.4	9.35	-	-	-	N: 0.089	Fe
H2 [14]	0.034	25.0	20.8	-	-	-	Si:0.5; P:0.016; S:0.002; Mn:0.74	Fe
T3F [15]	0.051	25.0	22.4	0.6	0.55	-	Si:0.23; P:0.005; S:0.002; Mn:1.17	Fe
T6 [14]	-	25.0	22.8	-	0.40	2.19	N:0.002; Si:0.25; Mn:1.43; Co:0.01; Nb:0.26	Fe
P92 [17]	0.12	9.0	-	-	-	0.3	W: 1.5	Fe
16Cr-4Al [18]	-	16.00	0.006	-	0.28	-	Al:4.59; Y:0.29; Y_2O_3:0.368; W 1.82	Fe
14YWT [19]	-	14.0	0.04	-	0.4	9.0	O:0.18	Fe
Inconel 625 [20]	-	22.0	Balance	-	-	9.0	Nb:3.5	Ni
Ti-15Mo-5Zr-3Al [21]	-	-	-	5.0	Balance	15.0	Al:3.0	Ti
Zircaloy-4	-	0.1	0.007	Balance	-	-	Sn:1.5; Fe:0.21	Zr
Zr-1.0Cr-0.2Fe [16]	-	1.0	-	Balance	-	-	Fe:0.2	Zr
Carpenter 20Cb-3	0.028	19.39	33.37	-	-	2.19	Si:0.33; P:0.023; S:0.004; Mn:0.4; Cu:3.2	Fe
AL6XN	0.02	20.4	23.85	-	-	6.21	N:0.22; Si:0.33; P:0.023; Mn:0.41; Cu:0.26	Fe
Nitronic 50	0.04	20.89	12.39	-	-	2.16	N:0.25; Si:0.48; P:0.025; S:0.009; Mn:5.14; V:0.16; Nb:0.17	Fe

3. Neutron Absorption By Materials

For a given level of fuel enrichment, the absorption of neutrons by in-core materials results in a reduction of the core reactivity. Higher absorbing in-core materials lead to the requirement for higher fuel enrichment, in order to reach the same exit burnup relative to a core with lower absorbing materials. Consequently, the choice of in-core materials will affect the reactor fuel efficiency and the overall sustainability of the fuel cycle. Below, relationships are derived between neutron absorption cross sections of in-core materials, their contribution to lattice cell reactivity and consequent impact on exit burnup.

3.1 The Microscopic and Macroscopic Absorption Cross Sections

Neutron absorption by materials is defined in terms of microscopic and macroscopic cross sections, σ_{abs} and Σ_{abs}, respectively. The former refers to absorption by a single atom or nucleus, while the latter refers to absorption by a material made up of N nuclei per m^3. The macroscopic cross section of a homogeneous mixture can be evaluated (see [23]) as

$$\Sigma_{\text{abs}} = \sum_{i=1}^{N} n_i \sigma_{abs,i} \,, \tag{2}$$

where n_{i} is the number of atoms of species i per m^3 and $\sigma_{abs,\,i}$ is the microscopic cross section in m^2 of species i. This expression can be rewritten in terms of material density and species weight fractions as

$$\Sigma_{\text{abs}} = \rho N_a \sum_{i=1}^{N} \frac{w_i \sigma_{abs,i}}{m_i} \,, \tag{3}$$

where ρ is the material density in kg/m^3, N_a is Avogadro's constant, w_{i}, $\sigma_{abs,\,i}$ and m_{i} are the weight fraction, microscopic cross section in m^2, and atomic weight in kg / mol, respectively, of species i. Table 2 (adapted from [23] and [24]) provides values for the thermal neutron microscopic and macroscopic cross sections for a variety of elements commonly found in the in-core alloys. Three strong neutron absorbers, B, Cd and Gd, are also included for comparison. The percent transmissions of thermal neutrons through 1 mm samples of the materials are also shown.

The candidate in-core alloys shown in Table 1 have as their majority chemical component: Fe, Ni, Ti, or Zr. Based on the data in Table 2, of these four elements, Ni is the highest neutron absorber, followed by Ti, then Fe, and finally Zr. Thus, qualitatively, and from the standpoint of fuel efficiency (i.e. neutron economy), Zr-based alloys are the best choice for in-core materials, followed by Fe, then Ti, and finally Ni-based alloys. Likewise, Fe-based alloys with low Ni content would provide better neutron economy than those with high Ni content. Since most alloys typically have several components, comparison of them requires an evaluation of their macroscopic thermal neutron absorption cross sections, Σ_{abs}. These can be evaluated using Equation 3 and the data provided in Table 2. Macroscopic cross sections, Σ_{abs}, were calculated for the alloys listed in Table 1, and are provided in Table 3. The percent transmissions of thermal neutrons through 1 mm samples of the alloys are also shown.

Table 2
Absorption cross sections (and related quantities) for elements commonly found in in-core alloy materials (adapted from [23] and [24])
(0.0253 eV Neutrons)

Atomic #	Element	σ_{abs} (10^{-28} m^2)	Atomic wt (AMU)	Density (kg/m^3) x 10^{-3}	Number density (m^{-3}) x10^{-28}	Σ_{abs} (m^{-1})	% Trans (1 mm)
5	B	767	10.8	2.35	12.81	9825.27	0.01%
6	C	0.0035	12.011	1.6	8.03	0.028105	100.00%
7	N	1.9	14.007	0.0013	0.0053	0.01007	100.00%
8	O	0.00019	15.999	0.0014	0.0053	0.000001007	100.00%
13	Al	0.231	26.982	2.699	6.02	1.39062	99.86%
14	Si	0.171	28.086	2.33	5	0.855	99.91%
15	P	0.172	30.974	1.82	3.54	0.60888	99.94%
16	S	0.53	32.064	2.07	3.89	2.0617	99.79%
22	Ti	6.09	47.90	4.51	5.67	34.5303	96.61%
23	V	5.08	50.942	6.11	7.21	36.6268	96.40%
24	Cr	3.05	51.996	7.19	8.33	25.4065	97.49%
25	Mn	13.3	54.938	7.43	8.15	108.395	89.73%
26	Fe	2.56	55.847	7.87	8.49	21.7344	97.85%
27	Co	37.18	58.933	8.90	8.99	334.2482	71.59%
28	Ni	4.49	58.71	8.90	9.13	40.9937	95.98%
29	Cu	3.78	63.54	8.96	8.49	32.0922	96.84%
39	Y	1.28	88.905	5.51	3.73	4.7744	99.52%
40	Zr	0.185	91.22	6.51	4.29	0.79365	99.92%
41	Nb	1.15	92.906	8.57	5.56	6.394	99.36%
42	Mo	2.48	95.94	10.20	6.4	15.872	98.43%
48	Cd	2450	112.40	8.65	4.64	11368	0.00%
50	Sn	0.626	118.69	7.00	3.4	2.1284	99.79%
64	Gd	49000	157.25	7.95	3.05	149450	0.00%
73	Ta	20.6	180.95	16.60	5.53	113.918	89.23%
74	W	18.3	183.85	19.30	6.32	115.656	89.08%
82	Pb	0.171	207.19	11.35	3.3	0.5643	99.94%

Table 3
Macroscopic Cross Sections of Candidate In-Core Alloys

Material	Density (kg/m^3)	Σ_{abs} (m^{-1})	% Trans (1 mm)
310 SS	8000	28.19	97.22%
304NG	8000	24.72	97.56%
H2	8000	27.16	97.32%
T3F	8000	28.20	97.22%
T6	8000	28.44	97.20%
P92	8000	22.97	97.73%
16Cr-4Al	7180	20.39	97.98%
14YWT	7180	21.36	97.89%
Inconel 625	8440	33.42	96.71%
Ti-15Mo-5Zr-3Al	4500	27.68	97.27%
Zircaloy-4	6560	0.88	99.91%
Zr-1.0Cr-0.2Fe	6440	1.04	99.90%
Carpenter 20Cb-3	8080	28.80	97.16%
AL6XN	8060	26.89	97.35%
Nitronic 50	7880	29.42	97.10%

3.2 Impact of Neutron Absorption on Reactivity

The primary objective of this report is to relate changes in reactivity and exit burnup to changes in neutron absorption due to in-core materials. This relationship is derived below, following a review of several key concepts regarding core and lattice reactivity.

The contribution of a device or material to the overall core reactivity is defined as its reactivity worth, $\Delta\rho$, which is simply the difference between the core reactivity before and after the device or material is inserted, given by

$$\Delta\rho = \rho_{\text{after}} - \rho_{\text{before}} . \quad (4)$$

In practice, the core reactivity and reactivity worths of various materials will depend in a complex way on the energy-dependent cross sections of the in-core materials, the energy-dependent cross sections of the fuel, the neutron spectrum and flux profile, and the core and lattice geometries. Nevertheless, it is possible to make some estimates of the impact of material neutron absorption cross sections on reactivity, relative to a reference case.

In Glasstone and Sesonske [23], an approximation is derived that relates a change in neutron absorption cross section to a resultant change in lattice or core reactivity. This approximation depends on the assumption that the lattice or core consists of a homogeneous mixture of materials. Although this assumption is clearly not true, it is useful for illustrative purposes. Based on this assumption, the absorption cross section of the lattice cell can be estimated using Equation 3 and can be separated into contributions from the various materials (e.g., fuel, cladding, liner tubes, etc.) in the cell as

$$\Sigma_{abs,cell} = \sum_{i=1}^{M} \frac{V_i}{V_{cell}} \Sigma_{abs,i} \,, \tag{5}$$

where V_{cell} is the volume of the lattice cell, M is the total number of materials present in the cell, and $\Sigma_{abs,i}$ and V_i are the macroscopic absorption cross section and volume, respectively, of material i. As discussed in [23], the reactivity difference in Equation 4 can be estimated from the corresponding change in macroscopic absorption cross section, given by

$$\Delta\rho \approx \frac{\Delta\Sigma_{abs}}{\Sigma_{abs}} \,, \tag{6}$$

where Σ_{abs} is the macroscopic absorption cross section of the cell prior to the change, and $\Delta\Sigma_{\text{abs}}$ is the value of the change in macroscopic absorption cross section. Equation 6 demonstrates that the impact of in-core materials on lattice cell reactivity, or reactivity change, $\Delta\rho$, relative to a reference case, is proportional to the corresponding $\Delta\Sigma_{\text{abs}}$ or change in lattice macroscopic absorption cross section.

Since different materials may have different physical properties, their volumes or thicknesses may differ in order to satisfy the same performance criteria. For example, cladding materials with lower tensile strengths may need to be thicker than those with higher tensile strength. When there is a difference between the volumes of material i and the reference material, then an additional material, δ, (e.g. coolant) must be either added or displaced to account for this difference. For comparison with the reference material, it is convenient to introduce the quantity $\Sigma_{\text{V, abs}}$, which is defined as the volume weighted average of the thermal cross sections of material i and the added or displaced material δ, given by

$$\Sigma_{V,abs} = \frac{V_i}{V_{REF}} \Sigma_{abs,i} + \frac{V_\delta}{V_{REF}} \Sigma_{abs,\delta} \,, \tag{7}$$

where $\Sigma_{abs,i}$ and $\Sigma_{abs,REF}$ are the macroscopic absorption cross sections of material i and of the reference material, respectively. V_i and V_{REF} are the volumes of material i and of the reference material, respectively. The macroscopic cross section of δ is $\Sigma_{\text{abs-}\delta}$, and its volume is defined to be

$$V_\delta = V_i - V_{REF} \,. \tag{8}$$

Equations 4 and 5 can then be combined to give

$$\Delta\rho \propto \Delta\Sigma_{abs} = \frac{V_i}{V_{REF}} \Sigma_{abs,i} - \frac{V_\delta}{V_{REF}} \Sigma_{abs,\delta} - \Sigma_{abs,REF} = \Sigma_{V,abs} - \Sigma_{abs,REF} \,. \tag{9}$$

In the special case where material i has the same volume as the reference material, Equation 9 reduces to

$$\Delta\rho \propto \Sigma_{abs,i} - \Sigma_{abs,REF} \,. \tag{10}$$

3.3 Neutron Absorption and Exit Burnup

Based on the linear reactivity model [22], the exit or discharge burnup, B_d, is proportional to the initial reactivity, ρ_0. Since reactivity is additive, B_d can then also be related, via Equation 9, to the change in-core material absorption cross sections as

$$B_d \propto \frac{V_i}{V_{REF}}\Sigma_{abs,i} + \frac{V_\delta}{V_{REF}}\Sigma_{abs,\delta} - \Sigma_{abs,REF} = \Sigma_{V,abs} - \Sigma_{abs,REF}\,. \tag{11}$$

In the special case where material i has the same volume as the reference material, Equation 11 reduces to

$$B_d \propto \Sigma_{abs,i} - \Sigma_{abs,REF}\,. \tag{12}$$

Thus, using the cross section data presented in Table 2 and Equations 3, 9 and 11, it is possible to compare and rank the impact on reactivity and exit burnup of various candidate in-core materials.

Note that the exit burnups, B_d, reported here are based on continuous refuelling. However, batch refuelling is also under consideration as a fuelling option for the CANDU SCWR [10]. The exit burnup, $B_{d,n}$ for a batch fuelled reactor is related to the continuous refuelled exit burnup, B_d by [22]

$$B_{d,n} = \frac{n}{n+1}B_d\,, \tag{13}$$

where n is the number of batches in a cycle.

4. Lattice Physics Results

4.1 The Effect of Alloy Composition

WIMS-AECL calculations were performed using the alloys listed in Table 1 as in-core materials. Equal volumes of material were used for the cladding and liner tubes in each case. The WIMS-AECL calculation results are summarized in Table 4, along with the thermal neutron absorption cross sections from Table 2. For these calculations, 310 stainless steel is used as a reference material, and so the absorption cross sections, reactivities and exit burnups are also shown relative to the corresponding reference values. The overall linear dependence of exit burnup on thermal neutron absorption cross section observed for the model materials is also seen for the candidate alloys. Figure 2 shows the calculated exit burnup as a function of change in thermal neutron absorption cross section relative to the 310 stainless steel reference case and corresponding linear fit to the data. These results confirm the predictions of Section 3.3 that, relative to a reference case, changes in exit burnup are approximately linear with changes to thermal absorption cross section. Therefore, qualitative ranking of materials with respect to their impact on exit burnup can be performed on the basis of their thermal neutron absorption cross sections, rather than requiring lattice physics calculations. Additional calculations (not shown) were performed using a different channel design, lattice pitch and fuel-type and confirm that this qualitative ranking does not depend on the details of the channel, bundle or lattice.

Table 4
Lattice Reactivity and Exit Burnup for Candidate In-Core Alloy Materials

Material	Σ_{abs} (m^{-1})	$\Delta\Sigma_{abs}$ (m^{-1})	Initial k-infinity	ρ_0 (mk)	$\Delta\rho_0$ (mk)	B_d (MWd/kg)	ΔB_d (MWd/kg)
310 SS	28.1892	0.00	1.28755	223.33	0	38.9	0
304NG	24.716	-3.4732	1.29867	229.98	6.65	40.4	1.5
H2	27.16	-1.0252	1.29062	225.1786	1.85	39.4	0.5
T3F	28.20	0.0097	1.28771	223.4276	0.10	38.9	0
T6	28.44	0.2516	1.28684	222.9026	-0.43	38.9	0
P92	22.9723	-5.2170	1.29695	228.96	5.63	40.4	1.5
16Cr-4Al	20.3902	-7.7991	1.304769	233.58	10.25	41.6	2.7
14YWT	21.36	-6.8312	1.29747	229.2693	5.94	40.1	1.2
Inconel 625	33.4216	5.2324	1.263109	208.30	-15.03	34.7	-4.2
Ti-15Mo-5Zr-3Al	27.6771	-0.5121	1.28814	223.69	0.36	39.3	0.4
Zircaloy-4	0.8812	-27.3080	1.375328	272.90	49.57	52.9	14.0
Zr-1.0Cr-0.2Fe	1.0401	-27.1491	1.374816	272.63	49.23	53.0	14.1
20Cb-3	28.80	0.6069	1.2836	220.9411	-2.39	38.3	-0.6
AL6XN	26.89	-1.2948	1.28677	222.8603	-0.47	38.90	0
Nitronic 50	29.42	1.2332	1.28123	219.5	-3.83	38.00	-0.9

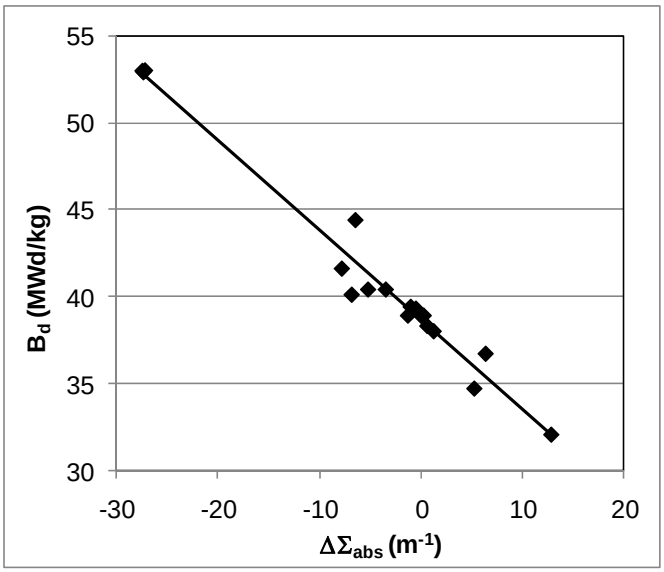

Figure 2 Calculated exit burnup versus $\Delta\Sigma_{abs}$ relative to 310 SS Reference

4.2 Impact on Reactivity and Burnup due to Changes in In-Core Material Volume

As discussed in Section 3.2, it is necessary to include the absorption cross section of material added or displaced to account for the material volume or thickness variation with respect to the reference material. For the system under investigation here, removing or adding (i.e. thinning or thickening) in-core material (e.g., fuel cladding or liner tubes) would be compensated by adding or removing coolant. The H_2O coolant, with a density of 0.19 g/cm^3, has a macroscopic thermal absorption cross section, $\Sigma_{abs,\delta}$, equal to 0.227 m^{-1}.

Table 5 shows the volume-weighted average thermal absorption cross sections for the SS 310 cladding as a function of thickness. The corresponding lattice reactivities and exit burnups evaluated using WIMS-AECL are also shown. Figure 3 shows a plot of the change in exit burnup as a function of change in volume weighted thermal neutron absorption cross section relative to the 0.3 mm 310 stainless steel reference case and corresponding linear fit to the data. These results further confirm the predictions of Section 3.3 that relative to a reference case, changes in exit burnup are approximately linear with changes to thermal absorption cross section. It is important to note, however, that in cases where changes in material volume displace or require addition of coolant, the thermal absorption cross section of the coolant must also be taken into account. Displacement or addition of coolant will also influence the coolant void reactivity, however, that effect is not considered here. Regarding the reactivity impact of materials, these results further support the notion that qualitative ranking of materials with respect to their impact on exit burnup can be performed on the basis of their thermal neutron absorption cross sections, rather than necessitating detailed lattice physics calculations.

Table 5
Volume-Weighted Average Thermal Absorption Cross Section, Lattice Reactivity and Exit Burnup for SS 310: Varying Cladding Thickness

Thickness (mm)	$\Sigma_{V,abs}$ (m^{-1})	$\Delta\Sigma_{V,abs}$ (m^{-1})	Initial k-infinity	ρ_0 (mk)	$\Delta\rho_0$ (mk)	Exit BU (MWd/kg)	ΔExit BU (MWd/kg)
0.1	20.84	-7.35	1.32500	245.28	21.95	45.20	6.26
0.2	24.29	-3.90	1.30616	234.40	11.07	42.09	3.16
0.3 (reference)	28.19	0.00	1.28755	223.33	0.00	38.93	0.00
0.4	32.54	4.35	1.26904	212.00	-11.33	35.72	-3.22
0.5	37.33	9.14	1.25073	200.47	-22.86	32.45	-6.48
0.6	42.57	14.38	1.23281	188.84	-34.49	29.63	-9.30

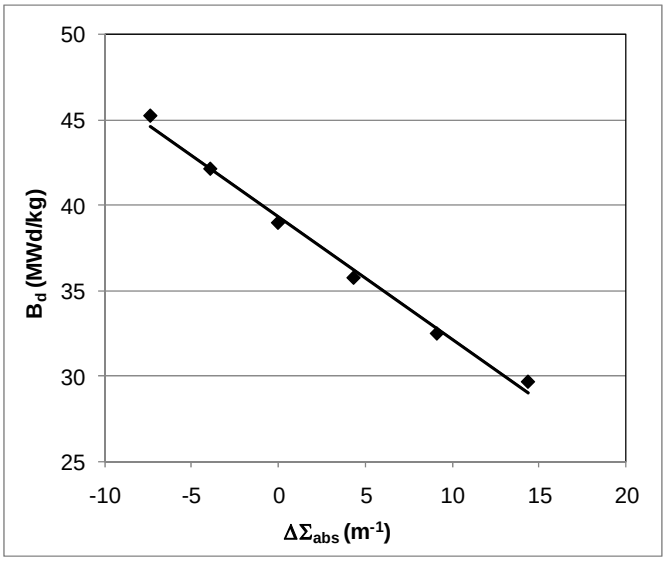

Figure 3 Calculated exit burnup versus volume-weighted absorption cross section difference relative to 0.3 mm cladding thickness

4.3 Estimation of Exit Burnup

The linear fits presented in Figure 2 and Figure 3 demonstrate that estimates can be made of the effect of in-core materials on exit burnup, based on their thermal absorption cross sections. In Figure 4, the data presented in Table 4 and Table 5 are combined in a single plot. Linear fits to the data sets are also shown. Although both data sets show an approximately linear dependence of exit burnup on $\Delta\Sigma_{abs}$, the actual slopes of the two fits are quite different. For materials having the same thickness, the exit burnup varies as

$$B_d = (-0.518 \pm 0.002)\Delta\Sigma_{abs} + (38.645 \pm 0.007). \quad (14)$$

When the thickness of 310 stainless steel is varied, the exit burnup follows

$$B_d = (-0.72 \pm 0.07)\Delta\Sigma_{abs} + (39.3 \pm 0.2). \quad (15)$$

The difference between these two results may be due to differences in the moderation of neutrons by light water coolant versus the alloy material. Consequently, a correlation used to predict impact on exit burnup from variation in materials of the same thickness cannot be used to predict changes to exit burnup due to cladding thickness changes, and vice versa. Nevertheless, for each scenario (changing material or changing thickness) it is possible to determine correlations that can be used estimate the impact on exit burnup. It is important to note that the constants describing these linear correlations (e.g in Equations 14 and 15) are likely to depend on the axial position, lattice cell, channel and bundle specifications. Consequently, changes to these specifications will likely require a re-evaluation of the fit parameters. Nevertheless, the trends, as discussed in Sections 4.1 and 4.2, are expected to be the same for any bundle, channel design or axial location along the channel (i.e. different coolant temperatures and densities).

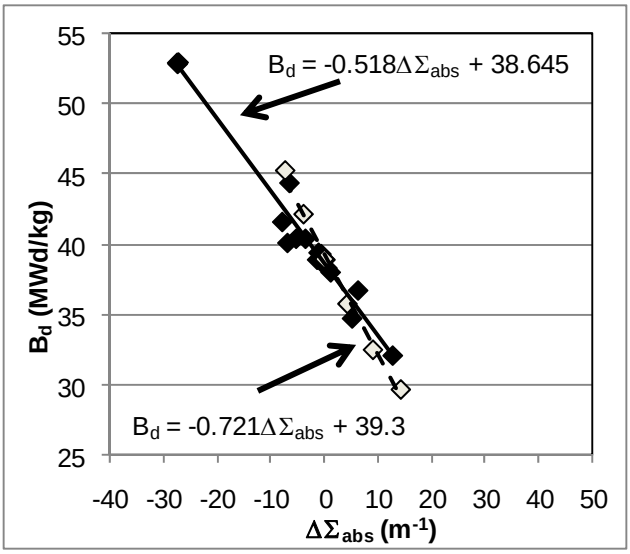

Figure 4 Exit burnup versus $\Delta\Sigma_{abs}$ relative to 310 SS reference

For various materials with the same volume, the correlation between exit burnup and $\Delta\Sigma_{abs}$ can be evaluated following the step-by-step procedure provided below.

1. The material chemical compositions and densities for a representative set of materials (including a reference material, e.g., 310 stainless steel) are used with Equation 3 and the data provided in Table 2 to obtain the corresponding macroscopic thermal neutron absorption cross sections, Σ_{abs}.
2. The relative thermal absorption cross sections, $\Delta\Sigma_{abs}$, for these materials are obtained by taking the difference $\Delta\Sigma_{abs} = \Sigma_{abs} - \Sigma_{abs,REF}$, where $\Sigma_{abs,REF}$ is the thermal absorption cross section of the reference material (e.g. 310 stainless steel). Note that these materials must have the same volume as the reference material.
3. The exit burnup is evaluated for the materials (and reference material) via a lattice physics calculation (e.g. using WIMS) and a linear fit of exit burnup versus Σ_{abs} is evaluated (e.g. Equation 14)**.**

5. Conclusions

It has been shown, using WIMS-AECL-based lattice cell physics calculations, that changes in exit burnup relative to a reference are proportional to changes in the macroscopic thermal neutron absorption cross section. These results demonstrate that qualitative ranking of materials with respect to their impact on fuel efficiency can be made based on their thermal neutron absorption cross sections as evaluated using Equation 3 and the data presented in Table 2. Furthermore, for a specific channel, lattice and bundle, estimates of exit burnup can be obtained via linear interpolation, as was done for the design here using Equations 14 and 15. Nevertheless, the qualitative assessment method for materials selection suggested here is not intended to replace evaluation via detailed physics calculations. Instead, it is intended that qualitative ranking of materials based on their impact on fuel efficiency will assist in identifying

those materials suitable for further materials testing and more detailed physics evaluation under SCWR conditions.

6. References

[1] U.S. DOE Nuclear Energy Research Advisory Committee and the Generation IV International Forum, "A Technology Roadmap for Generation IV Nuclear Energy Systems", GIF-002-00, 2002 December.

[2] R.B. Duffey, I.L. Pioro, and S. Kuran, "Advanced Concepts for Pressure-Channel Reactors: Modularity, Performance and Safety", *Journal of Power and Energy Systems*, Vol. 2, Iss. 1, 2008, pp 112-121.

[3] G.S. Was, P. Ampornrat, G. Gupta, S. Teysseyre, E.A. West, T.R. Allen, K. Sridharan, L. Tan, Y. Chen, X. Ren, and C. Pister, "Corrosion and Stress Corrosion Cracking in Supercritical Water", *Journal of Nuclear Materials*, Vol. 371, 2007, pp 176-201.

[4] K.L. Murty and I. Charit, "Structural Materials for Gen-IV Nuclear Reactors: Challenges and Opportunities", *Journal of Nuclear Materials*, Vol. 383, 2008, pp 189-195.

[5] D. Guzonas, P. Tremaine and J.-P. Jay-Gerin, "Chemistry Control Challenges in a Supercritical Water-Cooled Reactor", *Power Plant Chemistry*, Vol. 11, Iss. 5, 2009, pp 284-291.

[6] D. Guzonas, J. Wills, H. Dole, J. Michel, S. Jang, M. Haycock, and M. Chutumstid, "Steel Corrosion in Supercritical Water: An Assessment of the Key Parameters", The 2nd Canada-China Joint Workshop on Supercritical Water-Cooled Reactors (CCSC-2010), Toronto, Ontario, Canada, 2010 April 25-28.

[7] P. Yvon and F. Carré, "Structural Materials Challenges for Advanced Reactor Systems", *Journal of Nuclear Materials*, Vol. 285, 2009, pp 217-222.

[8] L. Zhang, F. Zhu and R. Tang, "Corrosion Mechanisms of Candidate Structural Materials for Supercritical Water-Cooled Reactor", *Frontiers of Energy and Power Engineering in China*, Vol. 3, Iss. 2, 2009, pp 233-240.

[9] D. Guzonas, "SCWR Materials and Chemistry: Status of Ongoing Research", Proceedings of the GIF Symposium, Paris, France, 2009 September 9-10.

[10] P.G. Boczar, W. Shen, J. Pencer, B. Hyland, P.S.W. Chan and R.G. Dworschak, "Reactor Physics Studies for a Pressure Tube Supercritical Water Reactor (PT-SCWR)", The 2nd Canada-China Joint Workshop on Supercritical Water-Cooled Reactors (CCSC-2010), Toronto, Ontario, Canada, 2010 April 25-28.

[11] C.K. Chow and H. F. Khartabil, "Conceptual Fuel Channel Designs for CANDU-SCWR", *Nuclear Engineering and Technology*, Vol. 40, Iss. 2, 2007, 139-146.

[12] D.V. Altiparmakov, "New Capabilities of the Lattice Code WIMS-AECL", PHYSOR 2008, International Conference on the Physics of Reactors, Nuclear Power: A Sustainable Resource, Interlaken, Switzerland, 2008 September 14 –19.

[13] H. W. Graves, Jr., "Nuclear Fuel Management", John Wiley & Sons, New York, 1979.

[14] S. Kasahara, J. Kaneda, Y. Tsuchiya, S. Mimura, M. Narui, M. Yamazaki, T.T. Shikama, and H. Matsui, "General Corrosion of Neutron Irradiated Candidate Alloys for Fuel Claddings of Supercritical Water-Cooled Reactor", 14th International Conference on Environmental Degradation of Materials in Nuclear Power Systems, Virginia Beach, Virginia, USA, 2009 August 23-27.

[15] Y. Tsuchiya, F. Kano, N Saito, M. Ookawa, and N. Hara, "Corrosion and SCC Properties of Fine Grain Stainless Steel in Subcritical and Supercritical Pure Water", Corrosion 2007, Nashville, Tennessee, March 11-15, 2007.

[16] A.T. Motta, A. Yilmazbayhan, M.J. Gomes da Silva, R.J. Comstock, G.S. Was, J.T. Busby, E. Gartner, Q. Peng, Y. H. Jeong, J.Y. Park, "Zirconium Alloys For Supercritical Water Reactor Applications: Challenges and Possibilities", *Journal of Nuclear Materials*, Vol. 371, 2007, pp 61-75.

[17] K. Yin, S. Qiu, R. Tang, Q. Zhang, and L. Zhang, "Corrosion Behaviour of Ferritic/Martensitic Steel P92 in Supercritical Water", Journal of Supercritical Fluids, Vol. 50, 2009, pp 235-239.

[18] A. Kimura, H.-S. Cho, N. Toda, R. Kasada, K. Yutani, H. Kishimoto, N. Iwata, S. Ukai, and M. Fujiwara, "High Burnup Fuel Cladding Materials R&D for Advanced Nuclear Systems: Nano-Sized Oxide Dispersion Strengthened Steels", *Journal of Nuclear Science and Technology*, Vol. 44, Iss. 3, 2007, pp 323-328.

[19] R.K. Nanstad, D.A. McClintock, D.T. Hoelzer, L. Tan and T.R. Allen, "High Temperature Irradiation Effects in Selected Generation IV Structural Alloys", *Journal of Nuclear Materials*, Vol. 392, 2009, pp 331-340.

[20] L. Tan, X. Ren, K. Sridharan and T.R. Allen, "Corrosion Behaviour of Ni-Base Alloys for Advanced High Temperature Water-Cooled Nuclear Plants", *Corrosion Science*, Vol. 50, 2008, pp 3056-3062.

[21] J. Kaneda, S. Kasahara, J. Kuniya, K. Moriya, F. Kano, N. Saito, A. Shioiri, T. Shibayama, and H. Takahashi, "General Corrosion Properties of Titanium Based Alloys for the Fuel Claddings in the Supercritical Water-Cooled Reactor", Proceedings of the 12th International Conference on Environmental Degradation of Materials in Nuclear Power System-Water Reactors. T.R. Allen, P.J. King and L. Nelson (eds.), TMS (The Minerals, Metals & Materials Society), 2005, pp 1409-1419.

[22] M.J. Driscoll, T.J. Downar, and E.E. Pilat, "The Linear Reactivity Model for Nuclear Fuel Management", American Nuclear Society, La Grange Park, Illinois, 1990.

[23] S. Glasstone and A. Sesonske, "Nuclear Reactor Engineering", Van Nostrand Reinhold Company, New York, 1981.

[24] V.F. Sears, "Neutron Scattering Lengths and Cross Sections", *Neutron News*, Vol. 3, Iss. 3, 1992, pp 26-37.